

Electronic Structure and the Fermi Surface of PuCoGa₅ and NpCoGa₅

Takahiro Maehira,¹ Takashi Hotta,¹ Kazuo Ueda,^{2,1} and Akira Hasegawa³

¹*Advanced Science Research Center, Japan Atomic Energy Research Institute, Tokai, Ibaraki 319-1195, Japan*

²*Institute for Solid State Physics, University of Tokyo, Kashiwa, Chiba 277-8581, Japan*

³*Niigata University, Niigata, Niigata 950-2181, Japan*

(Received 2 December 2002; published 23 May 2003)

Using a relativistic linear augmented-plane-wave method, we clarify energy band structures and Fermi surfaces of recently discovered plutonium-based superconductor PuCoGa₅ and the isostructural material NpCoGa₅. For PuCoGa₅, we find several cylindrical sheets of Fermi surfaces with large volume, similar to CeMIn₅, while for NpCoGa₅, the Fermi surfaces are found to be similar to those of UMGa₅. These similarities are discussed based on the *j-j* coupling scheme, suggesting some hints for the superconducting mechanism in HoCoGa₅-type *f*-electron compounds.

DOI: 10.1103/PhysRevLett.90.207007

PACS numbers: 74.25.Jb, 71.15.Rf, 71.18.+y, 74.70.Tx

Recently superconductivity has been discovered in PuCoGa₅ [1]. Surprisingly, the transition temperature T_c is 18.5 K, which is the highest among those yet observed *f*-electron materials and high enough even compared with other well-known intermetallic compounds. It has also been found that PuRhGa₅ becomes superconducting with $T_c = 8.7$ K [2]. These plutonium intermetallic compounds PuMGa₅ have the same HoCoGa₅-type tetragonal structure as CeMIn₅ [3]. Note that superconductivity occurs for $M = \text{Ir}$ ($T_c = 0.4$ K) and Co (2.3 K) in CeMIn₅, while antiferromagnetic (AF) phase has been found for $M = \text{Rh}$ at ambient pressure. Other isostructural materials including actinide ions are UMGa₅ [4] and NpCoGa₅ [5], but superconductivity has not been reported yet in both compounds. These HoCoGa₅-type compounds are frequently referred to as “115.”

Regarding the superconducting mechanism in the 115 compounds, first let us consider Ce-115. It has been widely considered that it is unconventional *d*-wave superconductor induced by AF spin fluctuations (see, for instance, Ref. [6]). In fact, there is some evidence such as T^3 behavior in nuclear relaxation rate [7] and node structure measured by thermal conductivity [8]. For the phase diagram of Ce(Co, Rh, Ir)In₅ [9], the AF state is found to exist adjacent to the superconducting phase. Concerning Pu-115, on the other hand, it is still premature to draw a definitive conclusion about the mechanism of superconductivity, but we envisage two scenarios: One is phonon-mediated conventional superconductivity, and the other is unconventional superconductivity with magnetic origin. From the experimental facts such as the Curie-Weiss behavior in magnetic susceptibility and electric resistivity in proportion to $T^{1.35}$ [1,2], spin fluctuations seem to play a crucial role also in Pu-115. Here we recall that *5f* electrons have an intermediate nature between localized *4f* and itinerant *3d* electrons. Namely, energy scale of *5f* electrons should be larger than that of *4f* electrons, paving a way to understand the higher T_c of Pu-115 if we assume the same electronic mechanism for superconductivity in Ce-115 and Pu-115.

However, irrespective of the mechanism, there is a question why Ce-115 and Pu-115 are superconductors, but U-115 and Np-115 are not. In the phonon mechanism, all HoCoGa₅-type materials can be superconducting. In the magnetic mechanism, U-115 and Np-115 can be superconducting with relatively high T_c similar to those of PuMGa₅, but that is not the case. Apparently some key issue is missing in the phonon mechanism and for the magnetic scenario, and it is not sufficient to consider U-115, Np-115, and Pu-115 as simple analogs to Ce-115 with large energy scale, based only on the difference in itinerant nature between *4f* and *5f* electrons. In order to get insights into the mechanism, first we need to clarify the difference and similarity among electronic structures of 115 materials.

In this Letter, we calculate energy band structures and Fermi surfaces for PuCoGa₅ and NpCoGa₅ by applying a relativistic linear augmented-plane-wave (RLAPW) method [10]. Then, we compare the results with those for CeMIn₅ [11] and UMGa₅ [4,12]. For PuCoGa₅, it is found that several sheets form cylindrical Fermi surfaces with large volume, similar to CeMIn₅ ($M = \text{Ir}$ and Co). For NpCoGa₅, we observe the Fermi-surface structure with large-volume part and several small pockets, similar to UFeGa₅ and UNiGa₅. The similarity between Ce-115 and Pu-115, as well as that between U-115 and Np-115, can be understood by the difference in *f*-electron number based on the *j-j* coupling scheme. We believe that the present results provide us with a couple of hints to consider the mechanism of superconductivity in 115 materials.

In our band-structure calculation, the local density approximation is used for the exchange and correlation potential, and the spatial shape of one-electron potential is determined in the muffin-tin approximation. Self-consistent calculations are performed by using the lattice constants determined experimentally [1,2].

In Fig. 1(a), we show the energy band structure for PuCoGa₅ along the symmetry axes in the Brillouin zone in the range from -0.5 to 1.0 Ryd. First note that in

the vicinity of the Fermi level E_F located at 0.446 Ryd, there occurs hybridization between Pu 5*f* and Ga 4*p* states. Above E_F near the *M* point, the flat 5*f* bands split into two groups, corresponding to the total angular momentum $j = 5/2$ (lower bands) and $7/2$ (upper bands). The magnitude of the splitting Δ between the two groups is estimated as $\Delta(\text{Pu}) = 1.0$ eV, which is almost equal to the spin-orbit splitting in the atomic 5*f* state of Pu. Note that each Pu APW sphere contains about 5.2 electrons in the *f* state, suggesting that the valence of the plutonium ion is Pu^{3+} , consistent with the experimental result [1].

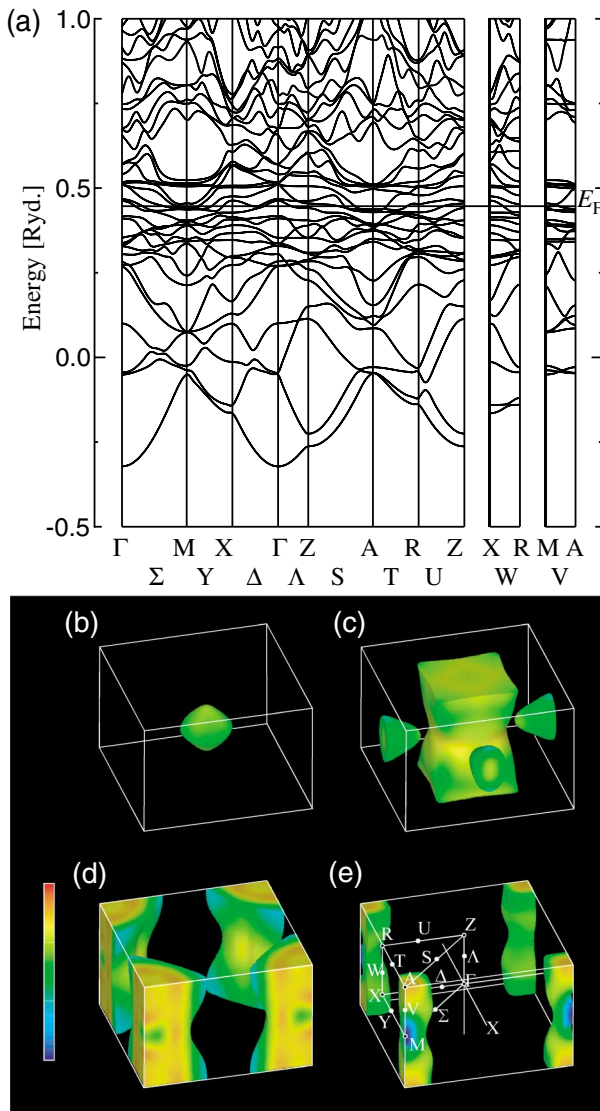


FIG. 1 (color). (a) Energy band structure for PuCoGa_5 obtained by the RLAPW method. Calculated Fermi surfaces of PuCoGa_5 for (b) 15th band hole sheets, (c) 16th band hole sheets, (d) 17th band electron sheets, and (e) 18th band electron sheets. Colors indicate the amount of 5*f* angular momentum character on each Fermi surface sheet and redshift indicates the increase of the *f* character. The center of the Brillouin zone is set at the Γ point.

207007-2

By using the total density of states at E_F , evaluated as $N(E_F) = 97.3$ states/Ryd cell, the theoretical specific heat coefficient γ_{band} is estimated as 16.9 mJ/K² · mol, while the experimental electronic specific heat coefficient γ_{exp} is 77 mJ/K² · mol [1]. If we define the enhancement factor for the electronic specific heat coefficient as $\lambda = \gamma_{\text{exp}}/\gamma_{\text{band}} - 1$, we obtain $\lambda = 3.6$, which is smaller than $\lambda = 10$ for CeCoIn_5 [11]. Note that the enhancement of λ from unity is a measure of electron correlation effect. The moderate λ in Pu-115 suggests that the correlation effect in Pu-115 should be weak compared with Ce-115. Since localized nature is stronger in 4*f* electrons, the correlation effect is more significant in Ce-115.

Now we discuss the Fermi surfaces of PuCoGa_5 . Since the lowest 14 bands are fully occupied, as shown in Fig. 1(a), the next four bands are partially occupied, while higher bands are empty. Then, as shown in Figs. 1(b)–1(e), the 15th, 16th, 17th, and 18th bands crossing the Fermi level construct the hole or electron sheets of the Fermi surfaces, summarized as follows: (i) The Fermi surface from the 15th band includes one small hole sheet centered at the Γ point. (ii) The 16th band constructs a large cylindrical hole sheet centered at the Γ point, while two equivalent small hole sheets are centered at *X* points. (iii) The 17th band has a large cylindrical electron sheet centered at the *M* point. (iv) The 18th band provides another cylindrical electron sheet centered at the *M* point. Among them, the main Fermi surfaces are determined from the viewpoints of the Fermi-surface volume and *f*-electron admixture. As for the Fermi surface constructed from the 18th band, *f* electrons are not uniformly distributed on it, as expressed in the color scale. Around the *A* point, the *f*-electron admixture is large, while the *p* electron gives a large contribution around the *M* point. If we ignore three dimensionality and small-volume Fermi surfaces, the main contributors are the hole sheet from the 16th band centered at the Γ point and the electron sheet from the 17th band centered at the *M* point.

Next let us make a comparison among the results for Ce-115 [11], U-115 [12], Np-115, and Pu-115. In Figs. 2(a)–2(d), we show the energy band structures around E_F for CeCoIn_5 , UCoGa_5 , PuCoGa_5 , and NpCoGa_5 , respectively. Note that CeCoIn_5 , UCoGa_5 , and PuCoGa_5 are compensated metals, while NpCoGa_5 is not. We estimate $\Delta(\text{Ce}) = 0.4$ eV, $\Delta(\text{U}) = 0.8$ eV, and $\Delta(\text{Np}) = 0.95$ eV, which are almost equal to the spin-orbit splittings in the atomic 4*f* and 5*f* states for Ce, U, and Np, respectively. As expected, we obtain $\Delta(\text{Ce}) < \Delta(\text{U}) \approx \Delta(\text{Np}) \approx \Delta(\text{Pu})$.

We note that the number to label the red and blue curves increases one by one among compensated metals in the order of CeCoIn_5 , UCoGa_5 , and PuCoGa_5 (see the caption of Fig. 2), corresponding to the increase in the *f*-electron number by two per site [see Fig. 2(a)]. Note also that the shapes of the red and blue curves among the three compounds are similar to one another, since overall band structure around the Fermi level is always

207007-2

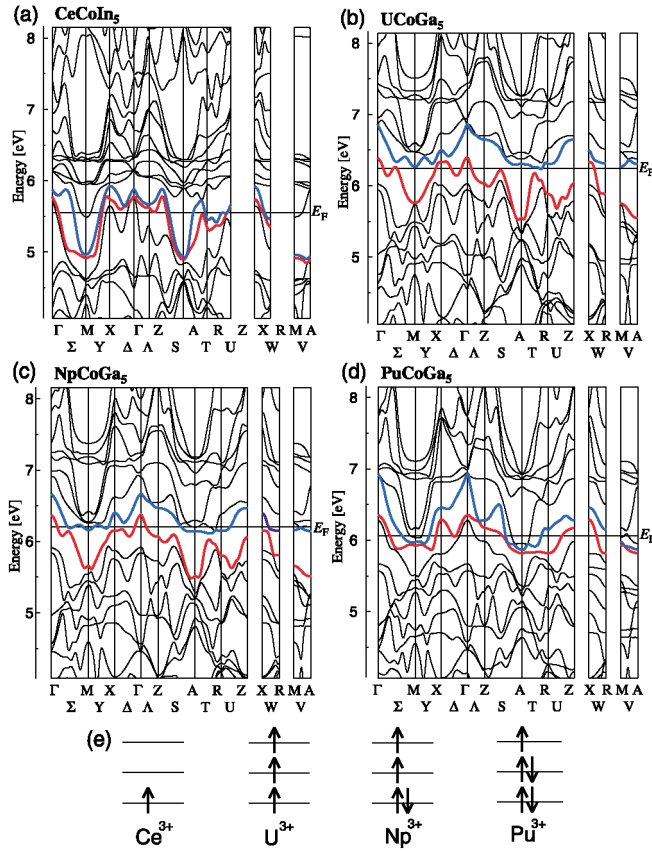


FIG. 2 (color). Energy band structure around E_F for (a) CeCoIn₅, (b) UCoGa₅, (c) NpCoGa₅, and (d) PuCoGa₅. In (a), (b), and (d), red and blue curves indicate the upper and lower bands to construct the hole and electron Fermi-surface sheets, respectively. Those are 14th (red) and 15th (blue) for CeCoIn₅, 15th (red) and 16th (blue) for UCoGa₅, and 16th (red) and 17th (blue) for PuCoGa₅. Note that for (c) NpCoGa₅, the bands to construct the two hole sheets, 15th and 16th, are specified by red and blue curves, respectively. (e) Configurations for f electrons accommodated in three Kramer's doublets. Up (down) arrow denotes pseudo-spin-up (-down).

determined by hybridization between broad p bands and narrow f bands for 115 compounds. For NpCoGa₅, the shapes of the 15th and 16th bands, denoted by the red and blue curves in Fig. 2(d), are almost the same as those of UCoGa₅. As deduced from Fig. 2(e), the Fermi level for NpCoGa₅ is shifted upward such that one f electron is added to UCoGa₅. Then, the volume of the Fermi surface from the 16th bands becomes large and the 17th band crosses the Fermi level to form small-pocket electron surfaces.

Let us note that the center of gravity of the $j = 5/2$ states in CeCoIn₅ is about 0.4 eV above E_F , while the center of those in PuCoGa₅ is slightly lower than E_F . Concerning UCoGa₅ and NpCoGa₅, the $j = 5/2$ states seem to be just at the Fermi energy. This trend is consistent with the number of f electrons in each compound. The spread of $j = 7/2$ and $5/2$ bands around the M or A points becomes broad in the order of CeCoIn₅, UCoGa₅,

and PuCoGa₅, while it is similar between UCoGa₅ and NpCoGa₅, consistent with the difference in $4f$ - and $5f$ -electron wave functions.

Here we emphasize that Ce-115 and Pu-115 exhibit large Fermi surfaces, as shown in Fig. 3(a) and Figs. 1(b)–1(e). In particular, we see a clear similarity between main Fermi surfaces of CeCoIn₅ and PuCoGa₅, except for fine structures. Considering only the f -electron dominant Fermi surface with a large volume, we observe in common the large hole sheet centered at the Γ point and the large cylindrical electron sheet centered at the M point. On the other hand, UCoGa₅ has small-pocket Fermi surfaces, as shown in Fig. 3(b) [12]. Namely, UCoGa₅ is considered as a semimetal, which seems to be closely related to the reason why UCoGa₅ does not exhibit superconductivity [13]. The semimetallic behavior may originate from slight overlap among the $j = 5/2$ f bands strongly hybridized with p states from Ga ions.

As shown in Fig. 3(c), the Fermi surfaces for NpCoGa₅ consists of small-pocket parts and a large-volume contribution. Note that the electronic state of NpCoGa₅ is similar to UCoGa₅ with one more f electron [see Fig. 2(e)]. Thus, the small-pocket parts are the remnants of UCoGa₅, while the large-volume Fermi surface contains one additional electron. Interestingly, the Fermi surfaces of UNiGa₅ [4] are quite similar to Fig. 3(c), since both UNiGa₅ and NpCoGa₅ are regarded as UCoGa₅ with one more electron, if we simply ignore the difference in the original character, d or f , of the additional one electron.

As discussed above, due to semimetal behaviors, it seems natural that superconductivity does not occur in UCoGa₅, but for NpCoGa₅, UNiGa₅, and UFeGa₅, a different reason should exist for the absence of superconductivity since there are large-volume Fermi surfaces. Here we notice that the number of cylindrical Fermi surfaces is

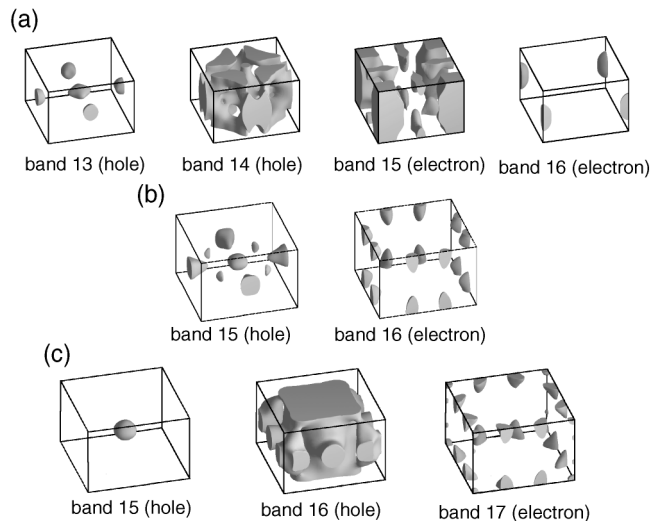


FIG. 3. Calculated Fermi surfaces of (a) CeCoIn₅, (b) UCoGa₅, and (c) NpCoGa₅.

one for UNiGa₅, UFeGa₅, and NpCoGa₅, while two (or three) sheets are observed for Ce-115 and Pu-115. Phenomenologically it seems that such multi-Fermi-surface structure originating from the multi-orbital nature of the *f* electron is a key issue for the appearance of superconductivity in 115 materials. It will be an interesting future problem to study this point based on a microscopic model.

Finally, let us discuss the similarity in energy band structures and Fermi surfaces between Ce-115 and Pu-115. First we point out the electron-hole conversion relation between Ce³⁺ and Pu³⁺ ions, as easily understood from Fig. 2(e). Note that this issue has been discussed for many years [14], but recently it has been refocused from the microscopic viewpoint for *f*-electron systems [15]. Thus, Pu-115 can be considered as a hole version of Ce-115, which is the very reason why common Fermi surfaces are observed. In order to confirm this picture, it is instructive to reanalyze the tight-binding model based on the *j-j* coupling scheme [15]. To consider the 115 systems, we include only *f* and *p* electrons in the two-dimensional network composed of Ce and In (Pu and Ga) ions. The Hamiltonian is given by the sum of *f*-electron hopping, *p*-electron hopping, and *f-p* hybridization terms, which are characterized by the Slater integrals (*ffσ*), (*ppσ*), and (*fpσ*), respectively. Note that crystalline electric field terms are simply ignored, since their energy scales are much smaller than the energies considered here.

In Fig. 4(a), we show the direct comparison between the RLAPW and tight-binding results for (*ffσ*) = 4500 K, (*fpσ*) = 6000 K, and (*ppσ*) = 18 630 K. The top and bottom of the tight-binding bands are determined by comparison with the RLAPW ones with a significant amount of Ga 4*p* states. The Fermi level for the tight-binding model is determined so as to include five *f* electrons. First, overall features of the bands in the vicinity of *E_F* are well reproduced by the mixture of broad *p* and narrow *f* bands. Second, magnitude of parameters for PuCoGa₅ are large compared with those for CeCoIn₅, (*ffσ*) = 4400 K, (*fpσ*) = 5360 K, and (*ppσ*) = 5730 K [11]. Note that the difference in (*ppσ*) between PuCoGa₅ and CeCoIn₅ is mainly due to the difference of Ga 4*p* and In 5*p* electronic states. Then, we conclude that 5*f* electrons are more itinerant than 4*f* ones from the present results for tight-binding fitting. As shown in Figs. 4(b)–4(d), the main Fermi surfaces are well reproduced by the tight-binding model. Good agreements between RLAPW and tight-binding results indicate the validity of the *j-j* coupling scheme for PuCoGa₅.

In summary, we have performed the band-structure calculation for PuCoGa₅ and NpCoGa₅. The Fermi surfaces for Pu-115 are similar to Ce-115 materials, and we have also observed a similarity between Np-115 and U-115. These similarities can be understood by the *f*-electron number difference based on the *j-j* coupling scheme. We believe that a way to understand supercon-

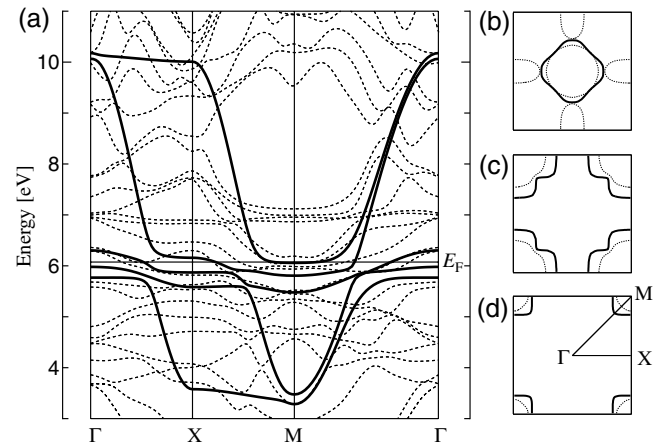


FIG. 4. (a) Energy band structures for PuCoGa₅ for the tight-binding model (solid curves) and the RLAPW results (dashed curves). Fermi surfaces discussed here are (b) 16th, (c) 17th, and (d) 18th band sheets. Solid and broken curves denote the tight-binding and RLAPW results, respectively.

ductivity in Pu-115 is to investigate the multi-orbital microscopic model by further adding Coulomb interactions.

We thank Y. Ōnuki, J. L. Sarrao, T. Takimoto, F. Wastin, and H. Yamagami for discussions. T.H. and K.U. are supported by the Grant-in-Aid for Scientific Research from Japan Society for the Promotion of Science.

Note added.—Fermi surfaces similar to our results were also obtained by Opahle and Oppeneer [16].

-
- [1] J. L. Sarrao *et al.*, Nature (London) **420**, 297 (2002).
 - [2] F. Wastin *et al.* (to be published).
 - [3] H. Hegger *et al.*, Phys. Rev. Lett. **84**, 4986 (2000); C. Petrovic *et al.*, Europhys. Lett. **53**, 354 (2001); C. Petrovic *et al.*, J. Phys. Condens. Matter **13**, L337 (2001).
 - [4] Y. N. Grin *et al.*, J. Less-Common Met. **121**, 497 (1986); Y. Ōnuki *et al.*, Acta Phys. Pol. B **32**, 3273 (2001); Y. Tokiwa *et al.*, J. Phys. Soc. Jpn. **70**, 2982 (2001); Y. Tokiwa *et al.*, J. Phys. Soc. Jpn. **71**, 845 (2002); H. Kato *et al.*, J. Phys. Chem. Solids **63**, 1197 (2002).
 - [5] P. Boulet *et al.* (private communication).
 - [6] T. Takimoto *et al.*, J. Phys. Condens. Matter **14**, L369 (2002); cond-mat/0212467.
 - [7] Y. Kohori *et al.*, Eur. Phys. J. B **18**, 601 (2000); G.-q. Zheng *et al.*, Phys. Rev. Lett. **86**, 4664 (2001).
 - [8] K. Izawa *et al.*, Phys. Rev. Lett. **87**, 057002 (2001).
 - [9] P. G. Pagliuso *et al.*, Physica (Amsterdam) **312-313B**, 129 (2002).
 - [10] M. Higuchi and A. Hasegawa, J. Phys. Soc. Jpn. **64**, 830 (1995), and references therein.
 - [11] T. Maehira *et al.*, J. Phys. Soc. Jpn. **72**, 854 (2003).
 - [12] T. Maehira *et al.*, cond-mat/0207575.
 - [13] UCoGa₅ is a Pauli paramagnet [4].
 - [14] B. R. Cooper *et al.*, Phys. Rev. Lett. **51**, 2418 (1983).
 - [15] T. Hotta and K. Ueda, Phys. Rev. B **67**, 104518 (2003).
 - [16] I. Opahle and P. M. Oppeneer, Phys. Rev. Lett. **90**, 157001 (2003).